



Metamaterial Based PIFA Antenna using Defective Ground Surface for handheld Applications

Tejaswi Jadhav¹, Namrata Walekar², Naziya Lakade³

Faculty, Department of Electronics Engineering, GRWPT, Sangli, India¹

Student, Department of Electronics Engineering, GRWPT, Sangli, India²

Student, Department of Electronics Engineering, GRWPT, Sangli, India³

Abstract: This paper describes a metamaterial-based broadband planar inverted-F antenna (PIFA) for handheld applications that uses a defective ground surface (DGS). The RIS (reactive impedance surface), which is made up of 3×3 square periodic structure of metallic unit cells, benefits the antenna's increased bandwidth. DGS is a technique for improving the antenna's variety of features, including size reduction and broad bandwidth. The proposed PIFA uses DGS and metamaterial to design, analyse, and fabricate a 2.4 GHz antenna. Finally, a prototype was simulated using the HFSS 3D electromagnetic simulator. The measured-10 dB S₁₁ impedance bandwidth design has been approximated to be 1199 MHz (2.0734-3.26921GHz), 49.95% of which at 2.4 GHz.

Keywords: PIFA, Metamaterial, RIS, Defective ground surface, Gain, Wideband. .

I. INTRODUCTION

Wireless communication's antenna function and design have recently progressed, resulting in an incredible expansion in handheld device subscribers. The service providers are paying more attention to their consumers' needs for lightweight, cost-effective antenna configurations. More improved communication capabilities, such as a broader frequency bandwidth or several frequency bands, became demanded by mobile users and equipment. On the other hand, these technologies need high-quality transmissions on both the transmitter and receiver sides. The most capable alternatives to this problem are increased gain and large bandwidth. The reduced size of a recent compact handset [1] allowed a significant number of antenna components. A basic low-profile PIFA with a wide tuning range [2]. PIFA is a fundamentally tunable lightweight antenna device with variable isolation enhancement for a portable phone, as shown in [3]. A printed-IFA with composite right/left-handed (CRLH) unit cells is examined in theory and practice using electromagnetic simulators. To further minimize the size of the antenna, capacitive loads are mounted to the open end of the L-loaded printed-IFA, and seven different printed components are merged into a compact handset [5], [6]. The linear polarized dual-band, single-layer, U-slot-fed antenna [7].

The symmetric slotted-slit microstrip patches of the RIS structure were employed to miniaturize the antenna while expanding bandwidth [8]. Metamaterial particles based on split-ring resonator research are used to boost the dispersion speed in a two-planar inverted-F antenna printed on a circuit board device [9]. The metamaterial is used for broad bandwidth in [10], [11], and DGS avoids coupling by adding currents in the reverse direction of the original characteristic modes (CM) currents described in [12]. In [13], the spacing between the patch and the ground plane can be minimized. In [14], metallic cross-branching enhanced the bandwidth of PIFA. PIFA is a robust and lightweight antenna with a tuneable internal antenna made of metamaterial [15]. Due to the demand for reduction gain enhancement, wireless communication systems have smaller antenna diameters. As a result, size reduction and bandwidth enhancement have become essential factors for PIFA mobile apps.

Two of PIFA's defining qualities are compact internal antennas for cell phones and ease of deployment. Because of its many attractive features, the PIFA is used in a variety of scenarios. However, some of the PIFA's shortcomings, such as power handling capacity, lower gain, polarization, and lesser bandwidth exceed the benefits. Precision analysis methodologies, superior principles, and optimal design techniques are required for bandwidth improvement.

This work provides a lightweight, wideband PIFA antenna based on RIS and DGS suitable for mobile devices and a small size. Because of PIFA's gain and decreased bandwidth, mobile communication is difficult. The antenna's bandwidth grows as the increase the height of the substrate and radiating patch. It has also resulted in a decrease in the efficiency factor. A new proposed metamaterial-based PIFA with DGS for smartphone devices is introduced to decrease the drawbacks of PIFA.

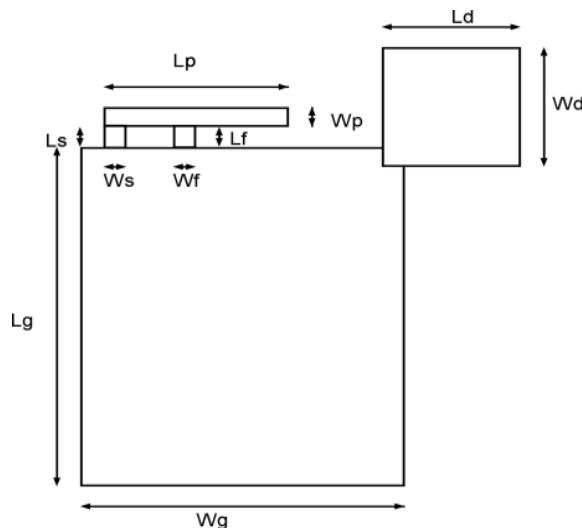


2.1 Conventional PIFA

In a typical PIFA, the top surface of the antenna is a radiating patch; the bottom surface is a ground plane, shorting pin, dielectric constant, and microstrip line feeding mechanism. An inverted-F antenna, which is structured like the letters F in English, serves as the primary antenna. The schematic structure of the proposed antenna is shown in Fig. 1. With a total designed volume of $24.01 \times 1.22 \times 2$ mm, the antenna is an appropriate ground plane. The ground surface of the PIFA antenna dimension is 56.4×51.3 mm on average. The overall ground surface dimension of the PIFA antenna is 56.4×51.3 mm. The antenna is built from a dielectric constant of 4.4 and a height of 1.59 mm of FR-4 substrate. Figures 1(a) and 1(b) depict the PIFA structure with DGS and a PIFA cross-section with RIS and DGS, respectively. The estimated dimensions of the PIFA with DGS are shown in Table 1. In the proposed antenna, two h_1 and h_2 dielectric substrates with heights of $h_1 = 1.59$ mm and $h_2 = 1$ mm are used.

I.1 Defective Ground Surface

A defective ground surface's basic structure is a square unit cell. A metallic square unit cell of DGS is attached with a side corner of the ground plane configuration of the antenna. As a result, the efficient inductive and capacitive components of the antenna's electric circuit current have an effect on the dielectric constant. The current distribution of the ground surface is affected by the defective surfaces with its slow-wave characteristic.



(a) PIFA with DGS

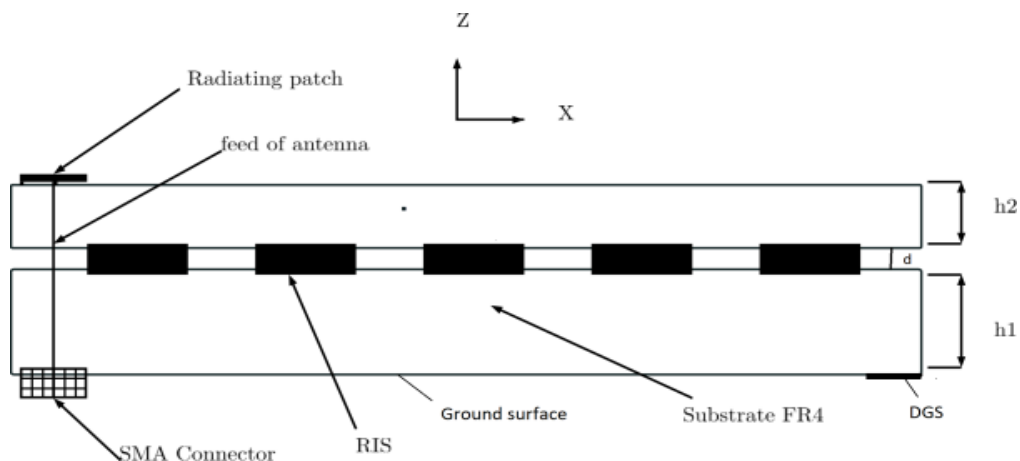


Fig. 1. Proposed PIFA using RIS and DGS



(b) Cross-sectional view proposed antenna

Electrical interference has been caused by the ground plane changing transmission line properties such as inductance and capacitance. In other words, a RIS and DGS-manipulated flawed or defected ground plane surface.

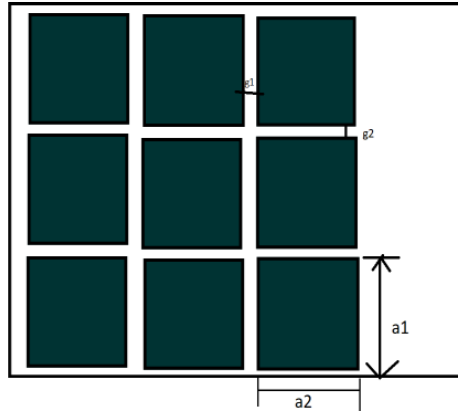


Fig. 2. Geometrical view of RIS

2.2 Reactive Impedance Surface

A PEC or PMC is used in the RIS to describe the total power while storing electric and magnetic energy. The lattice property of a resonant antenna is utilized to tune it below its natural resonance frequency. It shows RISs can reduce antenna-to-substrate interference, improving wideband operation and matching impedance. The performance of RIS improves the interface between the dielectric substrate and the radiating patch of the antenna. It also has an antenna with a front-to-back ratio analogous to that of a PEC surface. Fig. 2 shows the RIS structure as a periodic lattice of 3 × 3 array unit cells.

Table 1. Dimensions of Geometric parameters of PIFA with DGS antenna

Parameters	Size (mm)	Parameters	Size (mm)	Parameters	Size (mm)
D	1.0	g1	0.5	g2	0.3
Er	4.4	a1	16	a2	17
Ls	3.8	Wf	2.1	Lf	3.8
Ws	2.1	Lp	26.5	Wp	2.88
h1	1.0	Wg	51.3	Wd	20.63
h2	1.59	Lg	56.4	Ld	20.63

2.3 PIFA using RIS and DGS

The antenna geometrical dimensions of PIFA utilizing RIS and DGS are obtained by using various equations derived from the transmission line model. Optimal resonance frequency (Fr), dielectric substrate height (h), and substrate dielectric constant (r) are the three most important criteria to identify when developing a PIFA with RIS and DGS. The impedance bandwidth is equal to the thickness of the substrate and inversely proportional to the square root of the dielectric constant (εr) of the substrate. Calculated dimensions have been optimized using their corresponding frequency bands. The width of the patch is calculated using eq. 1 as follows.

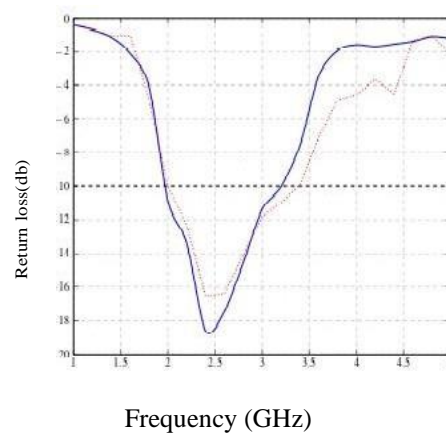
$$Wp = \frac{c}{2f \sqrt{\epsilon_{reff} + 1}} \quad (1)$$



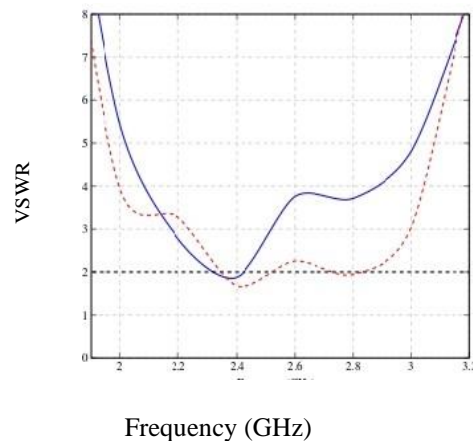
TM₁₀ mode is smaller than $\lambda/4$ in the fundamental mode, where λ is the wavelength of the dielectric medium and λ_0 is the wavelength of open space. In TM₁₀ mode, the field just changes with the length of $\lambda/4$ and is unaffected by patch distance. Where h is the height of the substrate, which is 1.59 mm, and the dielectric constant is 4.4. The length of the patch is calculated using eq.2 as follows

$$L_p = \lambda/4 \quad (2)$$

The PIFA antenna is mounted on a dielectric substrate which thickness is 4.4 and height 1mm. The designed antenna RIS structure is printed above the ground plane and a DGS square slot attached with the ground plane. A metallic slot with and length is smaller than 0.20λ . The dimensions of DGS are 20.63 mm in length and 20.63 mm in width, which are the same as the dimensions of the square slot. The antenna is then designed, manufactured, and tested.



(a) Measured and simulated Return Loss



(b) Measured and simulated VSWR

Fig. 3 Measured and simulate Results of Return Loss and VSWR of PIFA with RIS and DGS

III. EXPERIMENTAL RESULTS AND DISCUSSION

The PIFA with DGS geometry parameters are determined from the transmission line model's numerous equations. For WLAN bands at 2.4 GHz, the S₁₁ antenna design has a simulated-10 dB impedance bandwidth of 995 MHz (2.0734- 3.06921) 49.95 % and a measured-10 dB impedance bandwidth of 1199 MHz (2.0734-3.26921GHz) 41.45 %. The PIFA comprehensive testing employing RIS and DGS slightly improved in comparison to the simulated results of the performance parameters due to the air slit between the radiation component and the ground plane constructed during processing. For a smartphone application, the manufacturing antenna is very beneficial.

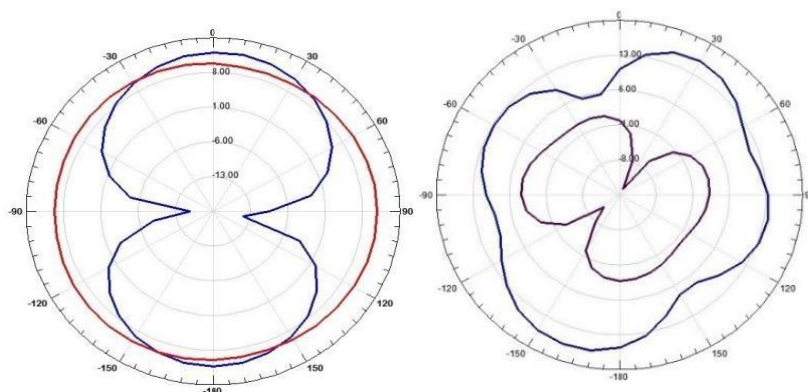
(a) $\Phi = 0$. (b) $\Phi = 90$.

Fig. 4. Radiation pattern of E Plane and H Plane

From the transmission line to the antenna, the proposed PIFA's measured VSWR is illustrated in Fig.3. (b). In the manufacturing process, the VSWR value was almost 1.69 at 2.4 GHz. It should be between 1 and 2, suggesting that the antenna is more efficient of E-Plane and H- Plane, respectively. In the XY plane, the simulated (co-polarized and cross-polarized) radiation pattern at 0° and 90° .

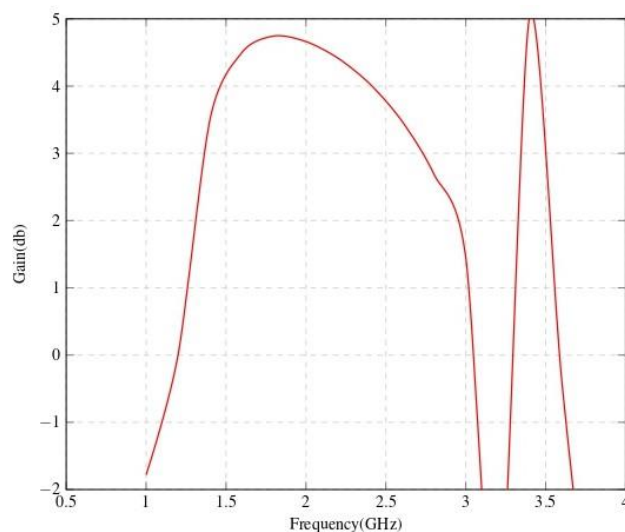


Fig. 5. Gain of proposed antenna

Fig.4 (a) and (b) illustrate the simulated radiation patterns. The simulated PIFA was simulated utilizing RIS and DGS configurations using the High-Frequency Structure Simulator. An antenna layout that has been optimized is referred to as "final designs." The feed has a connection with a grounding pin and a copper metal structure on the antenna's upper layer. The PIFA's microstrip feed point is a single wave port in the HFSS simulation. For calculation, the constructed prototype employs a SMA connector. SMA connections are female-type connectors.

The electrical properties of the structure are significantly influenced by the SMA connector. The EM simulation platform has been provided as an external link for real experimental validation. An extended probe runs through a hole on the lower surface of the antenna's substrate and attaches to the PIFA element's shorting pin to connect the PIFA element's microstrip feed location to the opposite end of the antenna.

The simulated gain of the PIFA for wireless devices employing RIS and DGS is as shown in Fig.5, which is acceptable and provides a superior wideband antenna gain is 4.03 dBi for 2.4 GHz.



IV. CONCLUSION

For WLAN applications, a Metasurface-based wideband PIFA with RIS and DGS. The proposed antenna's DGS might feature a regulated and wideband radiation pattern. The RIS structure is a lattice of 3×3 arrays of the surfaces of metallic patches, which aids in the antenna's bandwidth enhancement.

A 2.4 GHz antenna is created, analyzed, and implemented using the DGS PIFA with metamaterial. The approximated 1199 MHz impedance bandwidth based on WLAN bands at 2.4 GHz has a -10 dB impedance bandwidth (2.0734-3.26921GHz). In both simulated and manufactured results, PIFA using RIS and DGS produced radiation patterns, return loss, impedance bandwidth, gain, and VSWR response in the Wireless LAN application.

REFERENCES

- [1]. Kin-Lu Wong and Kai-Ping Yang. "Modified planar inverted f antenna", Electronics letters, 34(1):7-8, 1998.33
- [2]. Nguyen, V.A., Bhatti, R.A.Park, S.O (2008). A simple PIFA-based tunable internal antenna for personal communication handsets. IEEE Antennas and Wireless Propagation Letters, 7, pp.130-133.
- [3]. IJ Garcia Zuazola and John C Batchelor. "Compact multiband pifa type antenna", Electronics letters, 45(15):768-769, 2009.
- [4]. Soliman, A., Elsheakh, D., Abdallah, E., El-Hennawy, H. : Multiband printed metamaterial inverted-F antenna (IFA) for USB applications. IEEE Antennas and Wireless Propagation Letters, 14, 297-300. (2015).
- [5]. Dalia M Elsheakh and Esmat A Abdallah. "Compact multiband multifolded-slot antenna loaded with printed- ifa", IEEE antennas and wireless propagation letters, 11:1478-1481, 2012.
- [6]. Glogowski, R. Peixeiro, C (2008) Multiple printed antennas for integration into small multistandard handsets. IEEE Antennas and Wireless Propagation Letters, 7, pp.632-635.
- [7]. Liu, S., Qi, S.S., Wu, W. And Fang, D.G (2015) Single-feed dual-band single/dual-beam, Uslot antenna for wireless communication application. IEEE Transactions on Antennas and Propagation, 63(8), pp.3759-3764.
- [8]. Agarwal, K. Alphones, A(2013). RIS-based compact circularly polarized microstrip antennas. IEEE Transactions on Antennas and Propagation, 61(2), pp.547-554.
- [9]. Gil, I. Fernandez-García, R(2016), September. Study of metamaterial resonators for decoupling of a MIMO- PIFA system. In Electromagnetic Compatibility-EMC EUROPE, 2016 International Symposium on (pp. 552-556). IEEE.
- [10]. Lai, X.Z., Xie, Z.M., Cen, X.L. Zheng, Z (2013). A novel technique for broadband circular polarized PIFA and diversity PIFA systems. Progress In Electromagnetics Research, 142, pp.41-55.
- [11]. Dong, Y., Toyao, H. Itoh, T(2011). Compact circularly-polarized patch antenna loaded with metamaterial structures. IEEE transactions on antennas and propagation, 59(11), pp.4329- 4333.
- [12]. Ghalib, A. Sharawi, M.S(2017). TCM analysis of defected ground structures for MIMO antenna designs in mobile terminals. IEEE Access, 5, pp.19680-19692.DOI: 10.1109/ACCESS.2017.2739419
- [13]. Tejaswi Jadhav and Shraddha Deshpande. "Miniaturized planar inverted-f antenna with metallic cross branch for mobile communication", In 2019 International Conference on Intelligent Computing and Control Systems (ICCS), pages 617-620. IEEE, 2019.
- [14]. Tejaswi Jadhav and Shraddha Deshpande. "Planar inverted-f antenna using defected ground surface for mobile application", In ICDSMLA 2019, pages 611-619. Springer, 2020.
- [15]. Tejaswi Jadhav and Shraddha Deshpande. "Wideband circularly polarized planer inverted-f antenna using reactive impedance surface", International Journal of Innovative Technology and Exploring.2020.